

# CrystEngComm

Accepted Manuscript



This article can be cited before page numbers have been issued, to do this please use: P. Lucaioli, E. Nauha, I. Gimondi, L. Price, R. Guo, L. Iuzzolino, I. Singh, M. Salvalaglio, S. L. Price and N. Blagden, *CrystEngComm*, 2018, DOI: 10.1039/C8CE00625C.



This is an Accepted Manuscript, which has been through the Royal Society of Chemistry peer review process and has been accepted for publication.

Accepted Manuscripts are published online shortly after acceptance, before technical editing, formatting and proof reading. Using this free service, authors can make their results available to the community, in citable form, before we publish the edited article. We will replace this Accepted Manuscript with the edited and formatted Advance Article as soon as it is available.

You can find more information about Accepted Manuscripts in the [author guidelines](#).

Please note that technical editing may introduce minor changes to the text and/or graphics, which may alter content. The journal's standard [Terms & Conditions](#) and the ethical guidelines, outlined in our [author and reviewer resource centre](#), still apply. In no event shall the Royal Society of Chemistry be held responsible for any errors or omissions in this Accepted Manuscript or any consequences arising from the use of any information it contains.

## Serendipitous isolation of a disappearing conformational polymorph of succinic acid challenges computational polymorph prediction.

Received 00th January 20xx,  
Accepted 00th January 20xx

DOI: 10.1039/x0xx00000x

www.rsc.org/

Paolo Lucaioli<sup>a</sup>, Elisa Nauha<sup>a</sup>, Ilaria Gimondi<sup>b</sup>, Louise S Price<sup>c</sup>, Rui Guo<sup>c</sup>, Luca Iuzzolino<sup>c</sup>, Ishwar Singh<sup>a</sup>, Matteo Salvalaglio<sup>b</sup>, Sarah L Price<sup>c\*</sup>, Nicholas Blagden<sup>a\*</sup>

A conformational polymorph ( $\gamma$ ) of succinic acid was discovered in an attempt to purify a leucine dipeptide by cocrystallization from a methanol solution in the presence of various impurities, such as trifluoroacetic acid. The new  $\gamma$ -form was found to have crystallized concomitantly with the most stable  $\beta$  form. In light of this situation, a crystal structure prediction study was undertaken to examine the polymorph landscape. These studies reveal that the  $\gamma$  polymorph is thermodynamically competitive with the other observed polymorphs; having a more stable folded conformation than the planar crystalline conformation in the  $\beta$  form, but being stabilized less by the intermolecular interactions. Simulations and experiment show that the folded conformation is dominant in solution, but that trapping long-lived crystals of the new metastable polymorph may be challenging. Thus the  $\gamma$  polymorph provides a stringent test of theories for predicting which thermodynamically plausible structures may be practically important polymorphs.

### Introduction

Succinic acid (1,4-Butanedioic acid) is a biologically acceptable dicarboxylic acid that has been crystallized with many other molecules in attempts to develop cocrystals and salts with favourable physicochemical properties within the context of the crystal engineering of pharmaceutical dosage forms.<sup>1, 2</sup> Despite this, only two polymorphs containing just succinic acid have previously been reported, the  $\alpha$  form,<sup>3</sup> which is the most stable above 137 °C and can be obtained either by sublimation<sup>4</sup> or from the melt,<sup>5</sup> and the ambient stable  $\beta$  form.<sup>6</sup> In both of these polymorphs, like the majority of its crystal forms, the succinic acid molecule is planar, despite the high degree of conformational flexibility of the molecule.

In this contribution to the assortment of crystal forms of succinic acid, we report a new polymorph of succinic acid in a non-planar conformation, found concomitantly<sup>7</sup> with the stable  $\beta$  form, when succinic acid was investigated as a cofomer for the purification by cocrystallization of leucine dipeptide.<sup>8</sup> Thus succinic acid is another example of a molecule whose

polymorphism had appeared to have been established by extensive crystallization studies, but where a new polymorph is found in an attempted cocrystallization experiment.<sup>9-14</sup> The change in conformation, the concomitant crystallization and the subsequent unsuccessful attempts to reproduce the new polymorph, raise many questions about our ability to predict potential polymorphs.

### Results and discussion

#### The structures of the succinic acid polymorphs

The new succinic acid  $\gamma$  form crystallizes in space group C2/c with half a molecule of succinic acid in the asymmetric unit, in a markedly folded conformation. In the  $\gamma$  form, succinic acid molecules are connected with an  $R_2^2(8)$  carboxylic acid dimer hydrogen bonding motif ( $d(D\cdots A) = 2.662(2)$  Å) at each end of the molecule, yielding H-bonded chains running in the  $ac$ -direction (Figure 1b-c). These chains are connected to each other with weaker C-H $\cdots$ O hydrogen bonds (the shortest of which has  $d(D\cdots A) = 3.488(2)$  Å). It is notable that all three polymorphs contain the  $R_2^2(8)$  carboxylic acid dimer-linked chains, with the two symmetry independent chains in the  $\alpha$  polymorph and the chain in the  $\beta$  polymorph being virtually identical (Figure 1c), but notably in the  $\gamma$  form the succinic acid molecule is folded.

Analysis of all the crystal structures containing succinic acid in the Cambridge Structural Database shows that although the molecule is approximately planar in the vast majority (~89%) of crystal structures, there are still a number of cocrystals, solvates and salts featuring succinic acid in its folded conformation, with very high conformational similarity to the  $\gamma$  conformer (see ESI

<sup>a</sup> School of Pharmacy (PL, IS, NB), School of Chemistry (EN), University of Lincoln, Joseph Banks Laboratories, Green Lane, Lincoln, LN6 7DL, U.K.

<sup>b</sup> Thomas Young Center and Department of Chemical Engineering, University College London, Torrington Place, London, WC1E 7JE, U.K.

<sup>c</sup> Department of Chemistry, University College London, 20 Gordon St, London WC1H 0AJ, U.K.

†The crystal structure of the  $\gamma$  form is deposited as CCDC 1836394

The polymorph of monomethyl hydrogen succinate is noted in the ESI, and the structure has been deposited with the CCDC, CCDC1836683, as the details of crystal chemistry of this ester will be the subject of a separate publication.

Electronic Supplementary Information (ESI) available: Full details of the experimental and computational work. See DOI: 10.1039/x0xx00000x

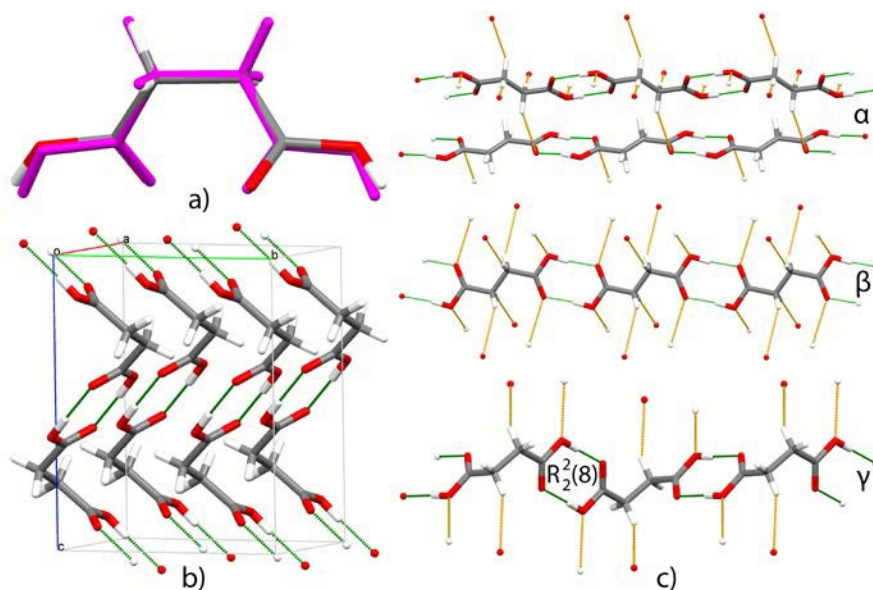


Figure 1. (a) Overlay of the molecular conformation in the conformational  $\gamma$  polymorph of succinic acid (coloured by element) with PBE0/6-31G(d,p) gas phase optimized conformation (magenta). (b) General packing diagram and unit cell of  $\gamma$  polymorph. (c) Comparison of the crystal structures of the three polymorphs of succinic acid, which all contain  $R_2^2(8)$  doubly hydrogen bonded chains (green bonds), that are planar in the  $\alpha$  and  $\beta$  polymorphs, but folded because of the conformation of the molecule in  $\gamma$ . Weaker C-H...O hydrogen bonding interactions shown in orange.

sections 1.5 and 1.6). In this analysis there is no appreciable difference in the density or void space between the succinic acid cocrystals, solvates and salts with the folded or planar conformation (ESI Tables S9-S11).

A conformational clustering analysis, performed through dSNAP,<sup>15</sup> shows a dozen folded conformations in cocrystals and that folded conformations can also be observed in hemisuccinates but only rarely in succinate salts (see ESI section 1.6). As shown in Figure 1a, *ab initio* conformational analysis of the isolated molecule (ESI)<sup>16</sup> shows that the folded conformation of succinic acid in the  $\gamma$  polymorph is very similar to the most stable conformation. The planar conformation of succinic acid is a local minimum in the conformational energy of the isolated molecule (ESI Figure S18). Its energy difference with respect to the folded

conformation varies with the computational method; however the application of density functional methods and larger basis sets (Figure S18) reduces significantly this conformational energy penalty from the 6 kJ mol<sup>-1</sup> which had been noted in an early rigid-molecule crystal structure prediction (CSP) study.<sup>16</sup> Within the crystal, different conformations of the molecule are capable of packing in different ways. The lattice energy  $E_{latt}$  is the sum of the intermolecular energy, summed over all interactions in the crystal, and the conformational energy penalty for distorting the molecule from its most favourable conformation. The compromise is reflected in the CSP study on succinic acid, which found a range of structures in between the highly metastable  $\alpha$  form and the  $\beta$  form, with the stability increasing with the density as shown in Figure 2.

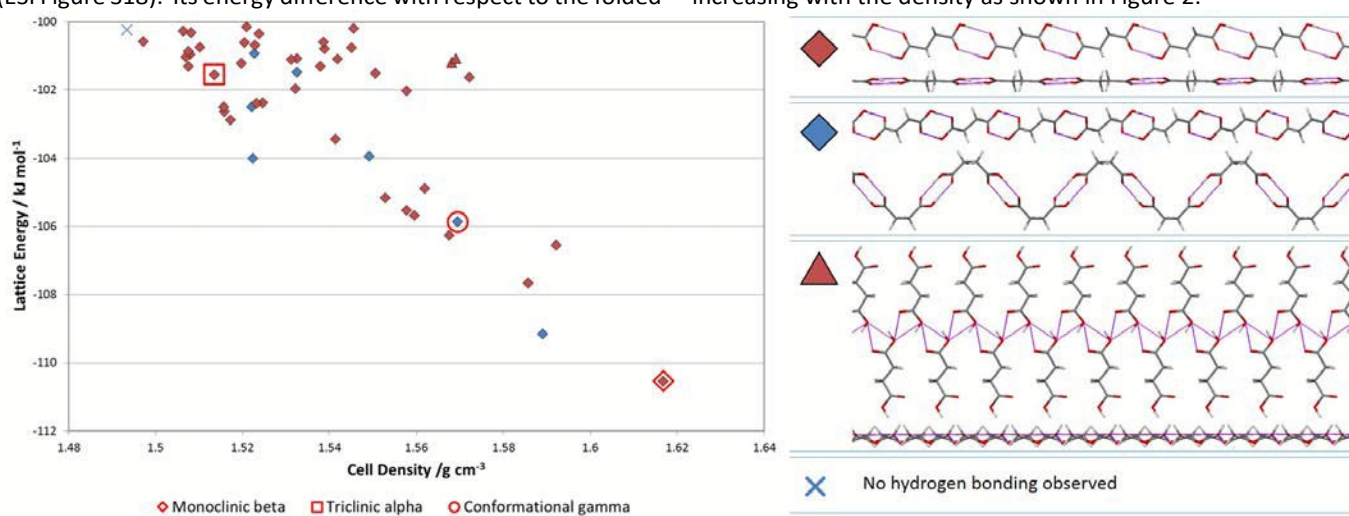


Figure 2. Summary of the CSP of succinic acid, where each symbol on the landscape represents a thermodynamically plausible crystal structure (lattice energy minimum). Colour denotes conformation type (red – planar, blue – folded) and shape denotes hydrogen bonding type, (with motif for diamond –  $R_2^2(8)$ , triangle –  $R_2^2(5)C_1^1(4)$ ) as shown.

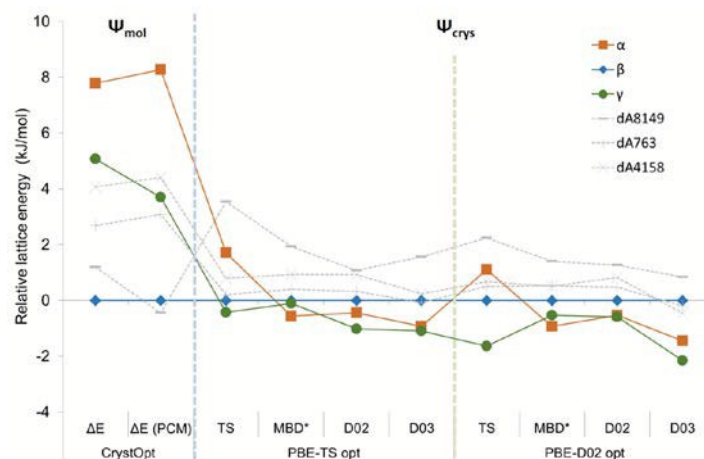


Figure 3. The lattice energies of the observed polymorphs and the three lowest energy unobserved CSP generated structures from Figure 2 relative to the  $\beta$  form, by (left)  $\Psi_{\text{mol}}$  calculations of the distributed multipoles and conformational energy contributions for the molecular geometry found using CrystalOptimizer in the CSP search from the molecular PBE0/6-31G(d,p) charge density of the isolated molecule, or within a polarizable continuum (PCM), and the FIT empirical repulsion-dispersion model and (right) by  $\Psi_{\text{crys}}$  DFT-D periodic electronic structure calculations, with various dispersion corrections, using the structures optimized at the PBE-TS and PBE-D02 level (see ESI section 3 for more detail.)

Among these were a few structures with the molecule in a non-planar conformation. The second most stable putative conformational polymorph was the new  $\gamma$  form. Furthermore, the CSP results suggest that there are other possible polymorphs of succinic acid, raising the question as to why we don't find even more polymorphs,<sup>17</sup> as well as why the  $\gamma$  form remained unreported for so long.

Additionally, CSP suggests that the new polymorph is metastable in lattice energy, but more stable than the  $\alpha$  form at low temperatures. Alternative models for the relative lattice energies, using periodic electronic structure calculations (DFT-

D, with the PBE functional, see ESI) (Figure 3), give smaller lattice energy differences, with  $\gamma$  slightly more stable than  $\beta$ , depending on the dispersion correction. The observed polymorphs are more stable than the hypothetical low energy structures from Figure 2. However, calculating the Helmholtz free energy stabilizes  $\beta$  such that  $\beta$  is more stable than  $\gamma$  at ambient temperatures (ESI Figure S22).

The adoption of a higher energy planar conformation of succinic acid in the  $\alpha$  and  $\beta$  forms raises the question whether this is the conformation of the molecule in solution in relation to any pre-nucleation ordering in solution. NMR analyses of the

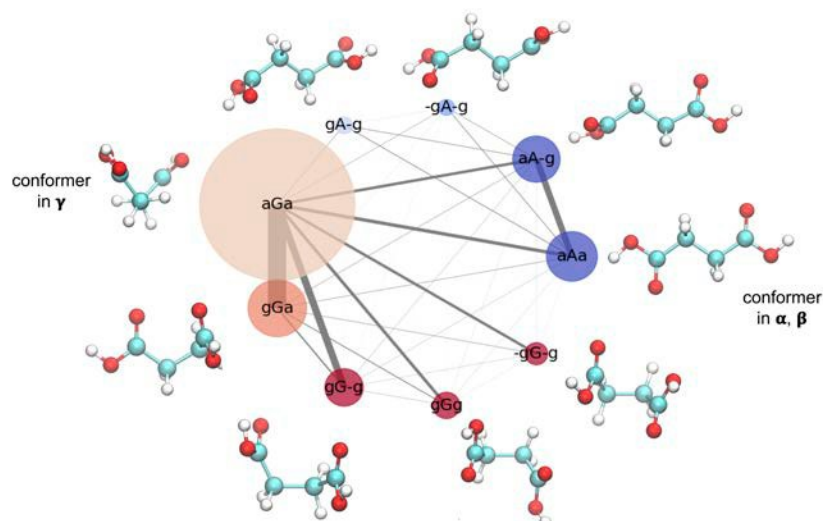


Figure 4. Results of MSM on unbiased MD on a molecule of succinic acid in water at 300 K. Network graph for the 9 gauche (shades of red) and anti (shades of blue) conformers. The size of the bubble corresponding to each graph is proportional to the overall time that the system spent with the specified conformational arrangement, whose molecular structure is shown the graph, while the definition of the labels associated to each conformer can be found in the ESI and Table S19. The conformer found in  $\gamma$  appears dominant in solution ( $67 \pm 3\%$ ), while the one found in  $\beta$  and  $\alpha$  ranks only third ( $7 \pm 1\%$ ). The width of the connections is weighted on the total number of conversions between the two conformers. These results come from the overall values of 18 unbiased MD simulations run for 100 ns.

conformation of succinic acid and its ions in solution<sup>18-20</sup> suggest that 80% of molecules are in a folded (gauche) conformation in methanol, more so in water, and less so in other alcohols. Early calculations of the conformations in both the gas phase and solution favour the folded conformation.<sup>21</sup> To further

characterize the conformational behaviour of succinic acid in water, we employed molecular dynamics (MD), well-tempered metadynamics (WTMetaD)<sup>22</sup> and the Markov State Model (MSM).<sup>23, 24</sup> In these simulations we explicitly include solute and solvent molecules, representing interactions with a classical



forcefield.<sup>25</sup> We find that the most stable conformer is aGa, corresponding to that observed in the  $\gamma$  polymorph, with a probability of 69±4% (WTMetaD, MSM 67±3%). The planar conformation (aAa), corresponding to that observed in the  $\alpha$  and  $\beta$  forms is the 3rd most probable conformer, with a probability smaller than 10%, corresponding to a solution free energy  $\square 3$  kJ mol<sup>-1</sup> less stable than aGa. However, the global relaxation time of the network of conformational states in solution is rather fast, of the order of 182 ps, showing that the conformations are fluctuating sufficiently rapidly that conformational change to form any of the polymorphs cannot be considered a rate-determining step to nucleation or growth.

The new metastable conformational polymorph appears to be thermodynamically plausible, and its conformation corresponds to the dominant conformation in solution. We attempted a wide range of experiments to reproduce finding the  $\gamma$  polymorph (ESI section 1.4) concentrating on the conditions in the original cocrystallization with leucine dipeptide that generated some single crystal(s) of  $\gamma$  amongst  $\beta$  succinic acid, and varying the component concentrations, using unpurified peptide, trifluoroacetic acid and the mono-methyl hydrogen succinate ester as the potential impurities. We were unable to find any single crystals of the  $\gamma$  form, confirming that its discovery was serendipitous and that it appears to be a “disappearing” polymorph.<sup>26</sup> The role of hetero-seeds or impurities as important in generating new crystal forms is becoming established, for example, a reproducible inability to

form a cocrystal of caffeine with paracetamol until fluoroparacetamol is added.<sup>27, 28</sup> Related surfaces can template new phases with common characteristics.<sup>29, 30</sup> Impurities can also impede the transformation to the more stable form.<sup>31</sup> In this instance it was not possible to identify an impurity which promotes the nucleation and growth of the  $\gamma$  polymorph concomitantly with the stable  $\beta$  form. (We note that a cocktail of impurities were found in a 50 year-old sample of a disappearing polymorph (form II) of progesterone<sup>32</sup> showing that impurity effects on crystallization can be impossible to reproduce.) Since trifluoroacetic acid was present, the ionization state of succinic acid could be varying, but an early NMR study<sup>20</sup> concluded that the folded conformation is more stable than the planar when pH  $\leq 5$  though there is a gradual change<sup>19</sup> in torsion angle with pH, but still favouring a folded conformation for the ions. The conformations in the observed salts of succinic acid (ESI Table S12) also suggest that local pH does not provide a simple explanation for the concomitant crystallization. The crystal morphology of  $\beta$  succinic acid is affected by a polymer additive,<sup>33</sup> showing that the growth kinetics are affected by the presence of other molecules. The conformational folding of the leucine dipeptide might aid the nucleation and growth of the  $\gamma$  form, altering the kinetic competition with the  $\beta$  form. However, nucleation is a stochastic process and it is possible that the  $\gamma$  form may have been overlooked or be below the concentration for detection (c.f. theophylline<sup>34, 35</sup>) in many crystallization experiments.

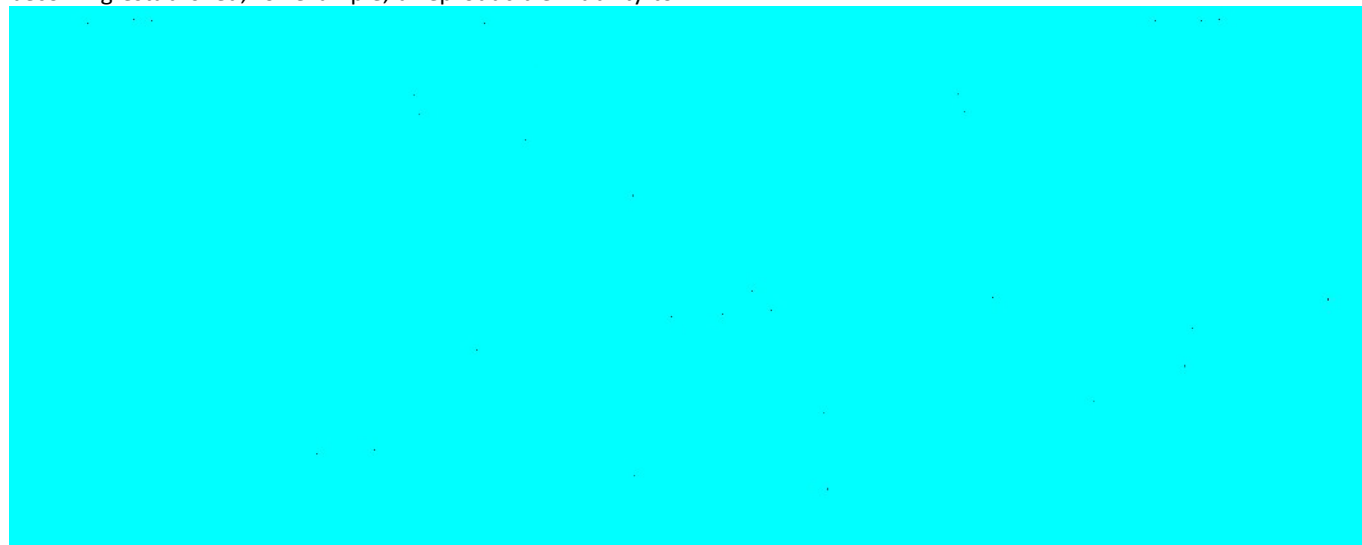


Figure 5. (a) Structural fluctuations of the  $\gamma$  polymorph at 300 K leading to melting. The experimental structure relaxes to a non-orthorhombic cell characterized by  $\beta=99^\circ$ . Enhancing fluctuations along  $\beta$  (displayed in green) with metadynamics allows us to reversibly sample the formation of a packing defect that leads to the local melting of the crystal structure. During this packing rearrangement conformational transitions to the planar conformer take place, leading to the observation of an irreversible melting transition that originates at the same layer involved in the appearance of a packing defect. (b) Free energy surface (FES) associated with the fluctuations in the crystal structure along  $\beta$  in the absence of structural defects. The FES has been obtained from Well-Tempered Metadynamics (details in the ESI). In red the estimate after 60 ns is reported; while in grey we highlight the range of variability of the free energy estimates obtained in the final 20 ns of simulation. It can be seen that the system gains  $\sim 3$  kJ mol<sup>-1</sup> per molecule due to the distortion of the  $\beta$  angle.

Performing classical MD simulations on the  $\beta$  and  $\gamma$  phases at 298 K shows that the  $\beta$  form is stable, with some transitory changes of the conformation. Adding thermal motion to simulate the  $\gamma$  form does not alter the conformation, though some global rearrangement of the experimental cell is observed. In particular, slippage of the hydrogen-bonded chains

leads to a lower energy structure with a  $\beta$  cell angle of approximately  $99^\circ$  (see Figure 5 and ESI section 4.3). This transformation in the periodic bulk representation of the  $\gamma$  polymorph used in MD simulations may be suggestive of real crystallites being susceptible to transformation to the more stable form. If the fluctuations shown in Figure 5 for slipping the

sheets of the  $\gamma$  form are enhanced through biased sampling with metadynamics (see ESI 4.3 for details), we observe defect formation, leading to the eventual melting of the structure. In a real  $\gamma$  crystal, the transformation to the  $\beta$  form is likely to nucleate at surfaces or defects, giving a crystal size dependence to the lifetime of  $\gamma$  crystals.

It seems likely that the crystallization of succinic acid is driven by thermodynamics favouring the flattening of the molecule as it crystallizes to the  $\beta$  form. Ostwald's rule of stages<sup>36</sup> might suggest that  $\gamma$  is an intermediate metastable phase that can form directly from solution, with the dominant conformation as the growth unit, and that we had serendipitously formed some large enough and perfect enough crystals that their size<sup>37</sup> and crystallinity prevented the transformation to the more stable  $\beta$  form (some crystals of which were found in the same vial).

As metastable polymorphs may have more desirable properties, such as higher solubility, or contaminate the phase purity of the desired polymorph, there is practical interest in understanding the formation of the  $\gamma$  polymorph. The high-temperature  $\alpha$  phase of succinic acid was once considered elusive at normal temperatures, but has been found as a contaminant after grinding<sup>38, 39</sup> and in liquid- (but not air-) segmented flow crystallization<sup>40</sup> or by spray-drying from water.<sup>41</sup> This suggests that the  $\alpha$  polymorph is observed when it forms first and there has not been sufficient time for the solvent mediated transformation. A similar hypothesis might also partially account for our inability to reproduce the formation of the  $\gamma$  form in solution crystallization with various impurities. (The impurities are likely to be necessary as it seems implausible that the  $\alpha$  form transforms to  $\gamma$  and then to  $\beta$  in an Ostwald's rule thermodynamic sequence if  $\alpha$  is less stable than  $\gamma$ .) The observation of  $\gamma$  succinic acid is highly plausible, both from the viewpoint of CSP and alternative thermodynamic models and the conformation in solution. The observation of  $\gamma$  succinic acid, with such a different conformation from the stable  $\beta$  form, provides a valuable, stringent test of our ability to understand and simulate the kinetic factors of nucleation, growth and transformation which determine which computer generated metastable crystal structures can be observed as metastable polymorphs.

## Conclusions

A conformational polymorph of succinic acid was found in an attempted purification of a peptide by cocrystallization, concomitant with the stable  $\beta$  form. The conformation in this  $\gamma$  form is the most stable for the isolated molecule and is the dominant conformation in solution, although the conformational change is very facile and rapid. The new form was predicted by a crystal structure prediction study. Periodic density functional calculations suggest that the  $\gamma$  form only becomes less stable than  $\beta$  through thermal effects. Molecular Dynamics simulations of the polymorphs suggest that the  $\gamma$  form is susceptible to transformation to the more stable  $\beta$  form, hence rationalising why we were unable to reproduce the crystallization of the  $\gamma$  form.

## Methods

### Experimental

**Peptide Synthesis and possible impurity profile.** The L-Leu-Leu-COOH dipeptide was synthesized through Fmoc Solid Phase Peptide Synthesis using Fmoc-NH Leu-OH protected amino acids (Merck Millipore) and 2-chlorotrityl resin (Iris Biotech GmbH). Initial loading was performed using 4 equivalents of protected amino acid and 8 equivalents of N,N-diisopropylethylamine (DIPEA) in dichloromethane. Deprotection steps were carried out using a 20% solution of piperidine in dimethylformamide (DMF). Fmoc-Leu-OH:HATU:DIPEA (4:4:8) in DMF was used for the coupling reaction while a 20:5:75 mixture of trifluoroacetic acid, triisopropylsilane and DCM was the cleavage cocktail (evaporated with a rotavapor). The material was freeze-dried to remove any possible moisture and to eliminate most of the unbounded trifluoroacetic acid.

**Co-crystallization experiment.** The L-Leu-Leu-COOH dipeptide in the lyophilized state and one equivalent of succinic acid (Tokyo Chemical Industries UK Ltd.) were dissolved using the minimum amount of methanol (HPLC grade) in separate vials. The dissolution of the powders was aided by stirring. The clear solutions were mixed, and the homogeneous liquid mixture was filtered to remove any possible source of heterogeneous nucleation. The vial containing the filtrate was capped with perforated parafilm to allow slow solvent evaporation at controlled temperature (20 °C) in an incubator. Crystals with dimensions suitable for single crystal X-ray diffraction were taken from the side and the base of the vial.

Many similar experiments were made to reproduce the formation of the  $\gamma$  polymorph, as detailed in the ESI. These included using increased peptide and trifluoroacetic acid, isolating separate contaminants, and introducing the ester as a potential reaction product.

**X-ray diffraction.** Single crystals suitable for X-ray diffraction measurements were mounted on MiTeGen Dual-Thickness MicroMounts and analyzed using a Bruker D8 Venture diffractometer with a Photon detection system. Unit cell measurements and data collections were performed at 173 K using a Mo K $\alpha$  radiation ( $\lambda = 0.71073 \text{ \AA}$ ). Crystal data and refinement parameters are presented in ESI Table S1.† Structure solutions were carried out by direct methods and refinement with SHELXL<sup>42</sup> was finished using the ShelXle<sup>43</sup> software.

### Computational

**Crystal Structure Prediction.** A revised<sup>16</sup> crystal structure prediction study was performed on succinic acid to cover all conformational space, using the programs CrystalPredictor2.2,<sup>44</sup> CrystalOptimizer2.4.4<sup>45</sup> and DMACRYS2.2.1.0<sup>46</sup> to generate a lattice energy landscape. The lattice energy in Figure 2 was calculated as the sum of the intermolecular energy (using a distributed multipole analysis<sup>47, 48</sup> of the PBE0/6-31G(d,p) charge density and FIT repulsion-dispersion parameters<sup>46</sup>) and an intramolecular energy penalty from the same charge density calculated by GAUSSIAN.<sup>49</sup> Full

View Article Online

DOI: 10.1039/C8CE00625C

details of the computational method, and other variations in the energy model including the periodic DFT-D calculations using CASTEP,<sup>50</sup> are given in the ESI.

**Molecular Dynamics Simulations.** Molecular Dynamics simulations were performed to analyse the conformational dynamics and thermodynamics of succinic acid in water and in the  $\beta$  and  $\gamma$  crystals. Well-Tempered Metadynamics (WTMetaD)<sup>22</sup> simulations instead have been performed to investigate the equilibrium distribution of conformers in solution, to analyse conformational transitions of single molecules in the bulk of the  $\beta$  phase and to compute the free energy surface associated with the distortion of the  $\gamma$  polymorph along the  $\beta$  angle (see Figure 5) of its crystallographic cell. Plain Metadynamics (MetaD)<sup>51</sup> simulations were carried out to investigate the destabilization of the  $\gamma$  polymorph induced by fluctuations along the  $\beta$  angle. In all cases succinic acid was modelled with GAFF,<sup>25</sup> while for water we used the TIP3P potential. All simulations were regulated at 300 K and 1 bar, using the Bussi-Donadio-Parrinello thermostat<sup>52</sup> and Berendsen barostat,<sup>53</sup> respectively. Further details of all the simulations, including additional analysis of the results are reported in the ESI. MD and WTMetaD simulations are carried out using Gromacs 5.2.1 patched with Plumed 2.3;<sup>54</sup> post-processing of the outputs employs Python,<sup>55, 56</sup> Visual Molecular Dynamics<sup>57</sup> (VMD) incorporated with GISMO,<sup>58</sup> and Plumed 2.3.<sup>54</sup>

### Conflicts of interest

There are no conflicts to declare.

### Acknowledgements

Profs Adjiman & Pantelides (Imperial College) for use of CrystalPredictor and CrystalOptimizer. Dr Anand N. P. Radhakrishnan for his support with Python coding, and Veselina Marinova for fruitful discussions on the implementation of the Markov State Models.

LI and IG acknowledge EPSRC (LI EP/GO36675/1, IG 1760926) and PL University of Lincoln strategic fund, for PhD scholarships. The CSP computational software is developed under EP/K039229/1. Periodic DFT calculations were performed on ARCHER, via our membership of the UK's HPC Materials Chemistry Consortium, which is funded by EPSRC (EP/L000202). The Molecular Dynamics calculations were performed on UCL Legion High Performance Computing Facility. MS, LSP and SLP are partially funded by Eli Lilly Digital Design.

### Notes and references

‡ Crystallographic data: Empirical formula  $C_4H_6O_4$ , Formula weight 118.09, Crystal system Monoclinic, Space group  $C2/c$ ,  $a/\text{\AA} = 5.7015(5)$ ,  $b/\text{\AA} = 8.4154(8)$ ,  $c/\text{\AA} = 10.3538(8)$ ,  $\alpha = 90^\circ$ ,  $\beta = 90.374(3)^\circ$ ,  $\gamma = 90^\circ$ ,  $V = 496.77(7) \text{\AA}^3$ ,  $Z = 4$ , Density (calculated) =  $1.579 \text{ Mg/m}^3$ , Absorption coefficient  $0.145 \text{ mm}^{-1}$ ,  $F(000) = 248$ , Crystal size  $0.143 \times 0.077 \times 0.023 \text{ mm}^3$ , Theta range  $3.936$  to

$29.202^\circ$ , Index ranges  $-7 \leq h \leq 7$ ,  $-11 \leq k \leq 11$ ,  $-13 \leq l \leq 14$ , Reflections collected 11388, Independent reflections 671,  $R(\text{int}) = 0.1089$ , Completeness to theta =  $25.242^\circ$  100.0 %, Max. and min. transmission 0.7458 and 0.6938, Data/restraints/parameters 671/0/40, Goodness-of-fit on  $F^2 = 1.095$ ,  $R1 [\text{I} > 2\sigma(\text{I})] = 0.0472$ ,  $wR2 [\text{I} > 2\sigma(\text{I})] = 0.0818$ , Largest diff. peak and hole  $0.317$  and  $-0.220 \text{ e.\AA}^{-3}$ .

### References

- R. D. B. Walsh, M. W. Bradner, S. Fleischman, L. A. Morales, B. Moulton, N. Rodriguez-Hornedo and M. J. Zaworotko, *Chemical Communications*, 2003, 186-187.
- N. Blagden, M. de Matas, P. Gavan and P. York, *Advanced Drug Delivery Reviews*, 2007, **59**, 617-630.
- I. M. Dodd, S. J. Maginn, M. M. Harding and R. J. Davey, personal communication.
- Q. Yu, L. Dang, S. Black and H. Wei, *Journal of Crystal Growth*, 2012, **340**, 209-215.
- G. D. Rieck, *Recueil Des Travaux Chimiques Des Pays-Bas*, 1944, **63**, 170-180.
- J. L. Leviel, G. Auvert and J. M. Savariault, *Acta Crystallographica Section B - Structural Crystallography and Crystal Chemistry*, 1981, **37**, 2185-2189.
- J. Bernstein, R. J. Davey and J. O. Henck, *Angewandte Chemie-International Edition*, 1999, **38**, 3440-3461.
- P. Lucaioli, E. Nauha, I. Singh and N. Blagden, *Crystal Growth & Design*, 2018, **18**, 1062-1069.
- G. M. Day, A. V. Trask, W. D. S. Motherwell and W. Jones, *Chemical Communications*, 2006, 54-56.
- M. Rafilovich and J. Bernstein, *Journal of the American Chemical Society*, 2006, **128**, 12185-12191.
- X. F. Mei and C. Wolf, *Crystal Growth & Design*, 2004, **4**, 1099-1103.
- B. Y. Lou, D. Bostroem and S. P. Velaga, *Crystal Growth & Design*, 2009, **9**, 1254-1257.
- P. Vishweshwar, J. A. McMahon, M. Oliveira, M. L. Peterson and M. J. Zaworotko, *Journal of the American Chemical Society*, 2005, **127**, 16802-16803.
- J. J. Li, S. A. Bourne and M. R. Caira, *Chemical Communications*, 2011, **47**, 1530-1532.
- G. Barr, W. Dong, C. J. Gilmore, A. Parkin and C. C. Wilson, *Journal of Applied Crystallography*, 2005, **38**, 833-841.
- N. Issa, S. A. Barnett, S. Mohamed, D. E. Braun, R. C. B. Copley, D. A. Tocher and S. L. Price, *CrystEngComm*, 2012, **14**, 2454-2464.
- S. L. Price, *Acta Crystallographica Section B: Structural Science, Crystal Engineering and Materials*, 2013, **69**, 313-328.
- J. D. Roberts, *Accounts of Chemical Research*, 2006, **39**, 889-896.
- G. Chidichimo, P. Formoso, A. Golemme and D. Imbardelli, *Molecular Physics*, 1993, **79**, 25-38.
- M. T. Nunes, V. M. S. Gil and J. Ascenso, *Tetrahedron*, 1981, **37**, 611-614.
- D. J. Price, J. D. Roberts and W. L. Jorgensen, *Journal of the American Chemical Society*, 1998, **120**, 9672-9679.
- A. Barducci, G. Bussi and M. Parrinello, *Physical Review Letters*, 2008, **100**, 020603.
- J. D. Chodera and F. Noe, *Current Opinion in Structural Biology*, 2014, **25**, 135-144.

24. J. H. Prinz, H. Wu, M. Sarich, B. Keller, M. Senne, M. Held, J. D. Chodera, C. Schutte and F. Noe, *Journal of Chemical Physics*, 2011, **134**, 174105.
25. J. M. Wang, R. M. Wolf, J. W. Caldwell, P. A. Kollman and D. A. Case, *Journal of Computational Chemistry*, 2004, **25**, 1157-1174.
26. D. K. Bucar, R. W. Lancaster and J. Bernstein, *Angewandte Chemie-International Edition*, 2015, **54**, 6972-6993.
27. D. K. Bucar, G. M. Day, I. Halasz, G. G. Z. Zhang, J. R. G. Sander, D. G. Reid, L. R. MacGillivray, M. J. Duer and W. Jones, *Chemical Science*, 2013, **4**, 4417-4425.
28. R. W. Lancaster, L. D. Harris and D. Pearson, *CrystEngComm*, 2011, **13**, 1775-1777.
29. C. C. Seaton, A. Parkin, C. C. Wilson and N. Blagden, *Crystal Growth & Design*, 2008, **8**, 363-368.
30. V. K. Srirambhatla, R. Guo, S. L. Price and A. J. Florence, *Chemical Communications*, 2016, **52**, 7384-7386.
31. N. Blagden and R. J. Davey, *Crystal Growth & Design*, 2003, **3**, 873-885.
32. R. W. Lancaster, P. G. Karamertzanis, A. T. Hulme, D. A. Tocher, T. C. Lewis and S. L. Price, *Journal of Pharmaceutical Sciences*, 2007, **96**, 3419-3431.
33. A. R. Klapwijk, E. Simone, Z. K. Nagy and C. C. Wilson, *Crystal Growth & Design*, 2016, **16**, 4349-4359.
34. D. Khamar, L. Seton, I. Bradshaw and G. Hutcheon, *Journal of Pharmacy and Pharmacology*, 2010, **62**, 1333-1334.
35. M. D. Eddleston, K. E. Hejczyk, A. M. C. Cassidy, H. P. G. Thompson, G. M. Day and W. Jones, *Crystal Growth & Design*, 2015, **15**, 2514-2523.
36. W. Z. Ostwald, *Zeitschrift fur Physikalische Chemie-International Journal of Research in Physical Chemistry & Chemical Physics*, 1897, **22**, 289-330.
37. A. M. Belenguer, G. I. Lampronti, A. J. Cruz-Cabeza, C. A. Hunter and J. K. M. Sanders, *Chemical Science*, 2016, **7**, 6617-6627.
38. V. Chikhaliya, R. T. Forbes, R. A. Storey and M. Ticehurst, *European Journal of Pharmaceutical Sciences*, 2006, **27**, 19-26.
39. A. V. Trask, N. Shan, W. D. S. Motherwell, W. Jones, S. H. Feng, R. B. H. Tan and K. J. Carpenter, *Chemical Communications*, 2005, 880-882.
40. K. Robertson, P. B. Flandrin, A. R. Klapwijk and C. C. Wilson, *Crystal Growth & Design*, 2016, **16**, 4759-4764.
41. K. M. Carver and R. C. Snyder, *Industrial & Engineering Chemistry Research*, 2012, **51**, 15720-15728.
42. G. M. Sheldrick, *Acta Crystallographica Section C-Structural Chemistry*, 2015, **71**, 3-8.
43. C. B. Hubschle, G. M. Sheldrick and B. Dittrich, *Journal of Applied Crystallography*, 2011, **44**, 1281-1284.
44. I. Sugden, C. S. Adjiman and C. C. Pantelides, *Acta Crystallographica Section B-Structural Science Crystal Engineering and Materials*, 2016, **72**, 864-874.
45. A. V. Kazantsev, P. G. Karamertzanis, C. S. Adjiman and C. C. Pantelides, *Journal of Chemical Theory and Computation*, 2011, **7**, 1998-2016.
46. S. L. Price, M. Leslie, G. W. A. Welch, M. Habgood, L. S. Price, P. G. Karamertzanis and G. M. Day, *Physical Chemistry Chemical Physics*, 2010, **12**, 8478-8490.
47. A. J. Stone, *Journal of Chemical Theory and Computation*, 2005, **1**, 1128-1132.
48. A. J. Stone, *GDMA: A Program for Performing Distributed Multipole Analysis of Wave Functions Calculated Using the Gaussian Program System*, 2010.
49. M. J. Frisch, G. W. Trucks, H. B. Schlegel, G. E. Scuseria, M. A. Robb, J. R. Cheeseman, G. Scalmani, V. Barone, B. Mennucci, G. A. Petersson, H. Nakatsuji, M. Caricato, X. Li, H. P. Hratchian, A. F. Izmaylov, J. Bloino, G. Zheng, J. L. Sonnenberg, M. Hada, M. Ehara, K. Toyota, R. Fukuda, J. Hasegawa, M. Ishida, T. Nakajima, Y. Honda, O. Kitao, H. Nakai, T. Vreven, J. A. Montgomery Jr., J. E. Peralta, F. Ogliaro, M. J. Bearpark, J. Heyd, E. N. Brothers, K. N. Kudin, V. N. Staroverov, R. Kobayashi, J. Normand, K. Raghavachari, A. P. Rendell, J. C. Burant, S. S. Iyengar, J. Tomasi, M. Cossi, N. Rega, N. J. Millam, M. Klene, J. E. Knox, J. B. Cross, V. Bakken, C. Adamo, J. Jaramillo, R. Gomperts, R. E. Stratmann, O. Yazyev, A. J. Austin, R. Cammi, C. Pomelli, J. W. Ochterski, R. L. Martin, K. Morokuma, V. G. Zakrzewski, G. A. Voth, P. Salvador, J. J. Dannenberg, S. Dapprich, A. D. Daniels, Ö. Farkas, J. B. Foresman, J. V. Ortiz, J. Cioslowski and D. J. Fox, *GAUSSIAN 09*, 2009.
50. S. J. Clark, M. D. Segall, C. J. Pickard, P. J. Hasnip, M. J. Probert, K. Refson and M. C. Payne, *Zeitschrift fur Kristallographie*, 2005, **220**, 567-570.
51. A. Laio and M. Parrinello, *Proceedings of the National Academy of Sciences of the United States of America*, 2002, **99**, 12562-12566.
52. G. Bussi, D. Donadio and M. Parrinello, *Journal of Chemical Physics*, 2007, **126**, 014101.
53. H. J. C. Berendsen, J. P. M. Postma, W. F. Vangunsteren, A. Dinola and J. R. Haak, *Journal of Chemical Physics*, 1984, **81**, 3684-3690.
54. G. A. Tribello, M. Bonomi, D. Branduardi, C. Camilloni and G. Bussi, *Computer Physics Communications*, 2014, **185**, 604-613.
55. M. F. Sanner, *Journal of Molecular Graphics & Modelling*, 1999, **17**, 57-61.
56. G. van Rossum, *Python: a computer language*, 1.5.1 edn., 1998.
57. W. Humphrey, A. Dalke and K. Schulten, *Journal of Molecular Graphics & Modelling*, 1996, **14**, 33-38.
58. M. Ceriotti, G. A. Tribello and M. Parrinello, *Proceedings of the National Academy of Sciences of the United States of America*, 2011, **108**, 13023-13028.